Mesenchymal Stem Cells-Derived Exosomal miR-223-3p Alleviates Ocular Surface Damage and Inflammation by Downregulating Fbxw7 in Dry Eye Models

Guifang Wang, Yujie Zhu, Yuzhen Liu, Mulin Yang, and Li Zeng

Ophthalmology Department, Loudi Central Hospital, Loudi, Hunan, China

Correspondence: Guifang Wang, Ophthalmology Department, Loudi Central Hospital, 51 Changqing Central Rd., Loudi, Hunan Province 417099, China; lafangme@ldzxyy.com.

Received: January 19, 2024
Accepted: September 5, 2024
Published: October 1, 2024

Citation: Wang G, Zhu Y, Liu Y, Yang M, Zeng L. Mesenchymal stem cells-derived exosomal miR-223-3p alleviates ocular surface damage and inflammation by downregulating Fbxw7 in dry eye models. *Invest Ophthalmol Vis Sci.* 2024;65(12):1. https://doi.org/10.1167/iovs.65.12.1

Purpose. Our previous study indicated that exosomes derived from mouse adipose-derived mesenchymal stem cells (mADSC-Exos) alleviated the benzalkonium chloride (BAC)-induced mouse dry eye model. However, the specific active molecules in mADSC-Exos that contribute to anti-dry eye therapy remain unidentified. In this study, we aimed to investigate the efficacy and mechanisms of miR-223-3p derived from mADSC-Exos in dry eye models.

Methods. Enzyme-linked immunosorbent assay (ELISA) experiments were conducted to determine miR-223-3p derived from mADSC-Exos that exerted anti-inflammatory effects on hyperosmolarity-induced mouse corneal epithelial cells (MCECs). The therapeutic efficacy of miR-223-3p was evaluated in mice with dry eye induced by either BAC or scopolamine (Scop). Mice were randomly assigned to 5 groups: sham, model, miR-223-3p overexpression, miR-223-3p knockdown, and 0.1% pranoprofen (positive group). Post-treatment, the severity of dry eye symptoms, and the pro-inflammatory cytokine levels were assessed. The effect of miR-223-3p on silencing the target gene was verified using ELISA and dual luciferase reporter assays.

Results. The mADSC-Exos that knocked out miR-223-3p did not reduce interleukin (IL)-6 content. Supplementing with miR-223-3p could restore the reduction of IL-6. The miR-223-3p effectively ameliorated ocular surface damage and decreased pro-inflammatory cytokines or chemokines in both BAC- and Scop-induced mouse dry eye models. Furthermore, miR-223-3p inhibited cell apoptosis. F-box and WD repeat domain-containing 7 (Fbxw7) was the potential direct target of miR-223-3p. The miR-223-3p suppressed the 3′-untranslated region of Fbxw7. The Fbxw7 knockdown suppressed hyperosmolarity-induced inflammation in MCECs.

Conclusions. The mADSC-derived exosomal miR-223-3p mitigates ocular surface damage and inflammation, indicating its potential as a promising treatment option for dry eye.

Keywords: mADSC-derived exosomal miR-223-3p, dry eye, Fbxw7, inflammation, ocular surface damage

Dry eye, a chronic ocular condition, is marked by destabilized tear film and an imbalanced ocular surface microenvironment, often leading to inflammation, tissue damage, and neurological issues.[1] The prevalence of dry eye is increasing, making it the most diagnosed issue in ophthalmology clinics, accounting for approximately 70% of all eye-related diseases. If left untreated, it can lead to severe inflammation and may result in blindness.[1,2] Mild dry eye due to insufficient tear secretion is typically treated with over-the-counter artificial tears. However, these are only effective for mild symptoms and may contain preservatives that can damage the cornea with frequent use. For moderate to severe dry eye with sufficient tear secretion, anti-inflammatory therapy becomes the primary treatment option. Although glucocorticoids act rapidly, they can increase intraocular pressure short-term and potentially lead to glaucoma with long-term use.

The etiology and pathogenesis of dry eye syndrome are complex and multifactorial, such as autoimmune disorders, environmental impacts, wearing of contact lenses, hormonal changes, chronic inflammation, infections, and iatrogenic factors.[3] Reduced tear secretion, altered tear film composition, and increased tear film evaporation contribute to ocular surface dryness, leading to epithelial damage and activation of inflammatory pathways. This triggers the release of pro-inflammatory cytokines and chemokines, attracting immune cells to the ocular surface, further exacerbating inflammation and perpetuating a vicious cycle.[4–6] In water-deficiency dry eye, reduced tear secretion increases tear film permeability, setting off an inflammatory cascade via mitogen-

activated protein (MAP) kinase and the nuclear factor-κB (NF-κB) signaling pathways.[7,8] Therefore, targeting inflammatory pathways represents a promising therapeutic strategy for managing dry eye, aiming to alleviate symptoms, restore tear film homeostasis, and promote ocular surface health.

MicroRNAs (miRNAs) are key in regulating gene expression, affecting inflammation, wound healing, and immune function.[9] In recent years, there has been an increasing body of research indicating that alterations in miRNAs could offer potential therapeutic targets for conditions such as dry eye syndrome.[9–11] Our previous study showed that exosomes from mouse ADSCs (mADSC-Exos) alleviate benzalkonium chloride (BAC)-induced dry eye in a mouse model by inhibiting the nucleotide-binding oligomerization domain (NOD)-like receptor family pyrin domain containing 3 (NLRP3) inflammasome.[12] However, the key active molecules in mADSC-Exos that contribute to anti-dry eye therapy remain unclear. The miR-223-3p, a key regulator of inflammation, reduces hyperosmolarity-induced inflammation by suppressing NLRP3 activation in patients with dry eye.[13–16] Furthermore, there was a significant correlation between the changes observed in miR-223-3p expression and the clinical and inflammatory parameters.[17] However, little is known about the therapeutic benefits and underlying molecular mechanism of miR-223-3p in the dry eye model. Understanding the function of miR-223-3p could provide new insights into the pathogenesis and potential therapeutic targets for dry eye disease.

Dry eye disease is classified into two distinct subtypes: quantitative (aqueous-deficient) and qualitative (evaporative). This study investigates the therapeutic potential of miR-223-3p in both subtypes of dry eye using mouse models. We used a quantitative model of dry eye induced by scopolamine (Scop)-mediated parasympathetic nerve blockage, mimicking reduced tear production, and a qualitative model induced by BAC, which replicates corneal epithelial damage and heightened inflammation. Furthermore, we explored the underlying mechanisms of miR-223-3p in hyperosmolarity-induced inflammation within mouse corneal epithelial cells (MCECs).

Materials and Methods

In Vitro Lentiviral Delivery of miR-223-3p Overexpression and Knockdown Construction

The pre-miRNA sequence of mouse miR-223-3p (Gene ID: 723814, MIMAT0000665) was connected into the NheI and BamHI restriction sites of FUGW-GSG-P2A-EGFP Lentivector (Addgene, Watertown, MA, USA). The short hairpin RNA (shRNA) target sequence of Mus musculus (mmu)-miR-223-3p was connected into the Bam H1 and EcoRI restriction sites of pGreenPuro (CMV) shRNA Cloning and Expression Lentivector (System Biosciences, Palo Alto, CA, USA). The pre-mmu-mir-223 sequence (MI0000703): 5′-UCUGGCCAUCUGCAGUGUCACGCUCCGUGUAUUUGACAAGCUGAGUUGGACACUCUGUGUGGUAGAGUGUCAGUUUGUCAAAUACCCCAAGUGUGGCUCAUGCCUAUCAG-3′; miR-223-3p shRNA sense strand, 5′-gatccTGGGGTATTTGACAAACTGACActtcctgtcagaTGTCAGTTTGTCAAATACCCCAtttttg-3', and anti-sense, 5′-AATTCAAAAATGGGGTATTTGACAAACTGACAtctgacaggaagTGTCAGTTTGTCAAATACCCCAg-3′.

Fbxw7 Overexpression or Knockdown Plasmid Construction

The Fbxw7 gene coding sequence (CDS; Gene ID: 50754, NM_001177774.1) was cloned into pcDNA3.1(+) vector (Thermo Fisher Scientific Inc., Waltham, MA, USA). The pcDNA3.1(+) vector was separately digested with NheI/EcoR. The shRNA targeting sequence for Fbxw7 was inserted into the AgeI and EcoRI restriction sites of pLKO.1-puro vector (Sigma-Aldrich, St. Louis, MO, USA). The recombinant plasmids, which were ligated with T4 DNA Ligase (New England Biolabs, Inc., Madison, WI, USA), were transformed into Escherichia coli and verified by sequencing. The primers used for PCR are listed as follows:

Forward: 5′-AGCTGGCTAGCGCCACCatgaatcagga-3′, Reverse: 5′-CTGCAGAATTCtcatttcatgtccac-3′, Fbxw7 shRNA sense strand, 5′-CCGGATCCGAAACCTCGTCACATTGCTCGAGCAATGTGACGAGGTTTCGGATTTTTTG-3′, and anti-sense, 5′-AATTCAAAAAATCCGAAACCTCGTCACATTGCTCGAGCAATGTGACGAGGTTTCGGAT-3′.

Experimental Animals

Specific-pathogen-free (SPF) grade male BALB/c mice (6 weeks, weighing 22–24 g) were purchased from Guangdong Yaokang Biotechnology Co., LTD. (License No. SCXK, Guangdong 2020-0054). BALB/c mice were kept in groups of 3 to 5 per cage, with unrestricted access to water and food, under a 12-hour light/dark cycle. The experimental protocols were approved by the Ethics Committee for Animal Experiments of Guangdong Zhiyuan Biomedical Technology Co., LTD.

Experimental Dry Eye Model

We established a mouse model of dry eye induced by BAC, following our previous study.[12] Briefly, the mice were administered 5 µL of 0.2% BAC (dissolved in sterile saline) 4 times daily at 1-hour intervals for 7 days. Thirty mice were randomly assigned into five groups ($n = 6$). These groups were as follows: sham group; model group; miR-223-3p overexpression group; miR-223-3p knockdown group; and a positive control group treated with 0.1% pranoprofen. Seven days following the treatment with BAC, the mice received an intraconjunctival injection of 1×10^6 viral genomes (vg) of lentivirus. Alternatively, the mice were administered 5 µL of 0.1% pranoprofen twice daily for a duration of 14 days.

Tear Breakup Time and Fluorescein Staining

On day 22, following the administration of anesthesia using 2.5% isoflurane, a 1% fluorescein solution was instilled into the conjunctival sac. The breakup time (BUT) was recorded in seconds under a slit lamp microscope (Haag-Streit Diagnostics, Wedel, Germany) after three complete blinks. This process was repeated three times for each eye, with the average value taken as the result. Then, fluorescein staining was performed. The corneal surface was then examined using a slit lamp microscope and was divided into four quadrants for detailed assessment. Each quadrant was evaluated and scored based on the extent of fluorescein staining, with the scores summed to obtain a total for each eye. The scoring criteria were as follows: score 0 = no fluorescence; score 1 = slight fluorescence resembling sparse dots; score 2 = dense dot-like pattern of fluorescence; score 3 = very dense dot-

Investigative Ophthalmology & Visual Science

like fluorescence; and score 4 = positive fluorescein plaque formation.[18]

Tear Volume Measurement

The tear volume measurement was performed on day 22 according to our previous study.[12] Briefly, the tear volume was quantified utilizing phenol red-impregnated cotton threads (Zone-Quick, Yokota, Tokyo, Japan). The lower eyelid was gently retracted, and a 1-mm segment of the thread was positioned on the palpebral conjunctiva for a duration of 15 seconds. The length of the wetted portion of the thread was then measured in millimeters. This measurement process was repeated three times per eye, and the mean value of these measurements was recorded as the final tear volume.

Hematoxylin and Eosin Staining

Upon completion of the experiment, the mice were euthanized using isoflurane. The eyeballs were extracted and fixed in an ocular fixative for 24 hours. Following fixation, the eyeballs underwent gradient ethanol dehydration, xylene clearing, and paraffin infiltration to preserve the tissue for subsequent analysis. The sections (5-µm thick) were stained using the hematoxylin and eosin (H&E) staining kit (Solarbio, Beijing, China) according to the manufacturer's protocols. Representative H&E staining images were captured using a conventional light microscope (Olympus, Tokyo, Japan).

Periodic Acid-Schiff Staining

The sections were stained with the Periodic Acid-Schiff (PAS) staining kit (Solarbio, Beijing, China) according to the manufacturer's protocols. Representative images of the conjunctiva were captured with a conventional light microscope (Olympus, Tokyo, Japan). The number of goblet cells in the conjunctiva were counted from three eyes per group.

Immunohistochemistry

Sections were incubated in the anti-MUC5AC primary antibody (1:200, sc-21701; Santa Cruz, CA, USA) for 24 hours at 4°C, washed in PBS, and incubated with secondary anti-rabbit-HRP antibody. Immunostaining was visualized using 3, 3′-diaminobenzidine (DAB) substrate (Vector Laboratories, Burlingame, CA, USA) and images were captured with a conventional light microscope (Olympus, Tokyo, Japan).

Terminal Deoxynucleotidyl Transferase dUTP Nick-End Labeling Assay

The TUNEL assay was performed according to the manufacturer's instructions (Roche, Basel, Switzerland). For each treatment group, TUNEL-positive cells were counted in 3 random fields under a microscope (Olympus, Tokyo, Japan) at 200 × magnification.

Cell Culture and Treatment

The immortalized MCECs and mADSC were acquired from the American Type Culture Collection (ATCC, Manassas, VA, USA). MCECs and mADSC were cultured in Procell complete medium (Wuhan, China) and in a complete stem cell culture medium, respectively. Hyperosmotic stress was induced using hyperosmotic growth media (500 mOsm/kg by NaCl addition).

MCECs cells (2.5×10^5 cells/well) were plated into 6-well plates for 24 hours, and then incubation with different multiplicity of infection (MOI) of FUGW-miR-223-3p-GSG-P2A-EGFP or pGreenPuro siRNA-anti-miR-223-3p or transiently transfected with 0.5-2 µg Fbxw7 overexpression or knockdown plasmid for another 48 hours. Following the treatment, the supernatants from the culture medium were collected for analysis through Western blot analysis.

MCECs cells (2.5×10^5 cells/well) were seeded into 6-well plates and added FUGW-miR-223-3p-GSG-P2A-EGFP or pGreenPuro siRNA-anti-miR-223-3p or transiently transfected with 2 µg Fbxw7 overexpression or knockdown plasmid for 48 hours. MCECs cells were then incubated with 500 mOsm/kg hyperosmotic growth media for another 24 hours, the supernatants from the culture medium were then gathered for interleukin (IL)-6, IL-1β, and tumor necrosis factor (TNF)-α (all in pg/mL) analysis using enzyme-linked immunosorbent assay (ELISA).

MCECs cells (2.5×10^5 cells/well) were seeded into 6-well plates and added pGreenPuro siRNA-anti-miR-223-3p and/or FUGW-miR-223-3p-GSG-P2A-EGFP or mADSC-Exos (10 µg/mL) for 48 hours. MCECs cells were then incubated with 500 mOsm/kg hyperosmotic growth media for another 24 hours. Following the treatment, the supernatants from the culture medium were collected specifically for the analysis of IL-6 levels.

The mADSCs (1×10^6 cells/well) were seeded into 10 cm culture dishes and added pGreenPuro siRNA-anti-miR-223-3p for 48 hours. The isolation of miR-223-3p knock out-containing mADSC-Exos in supernatant was performed according to our previous study.[12] The MCECs cells (2.5×10^5 cells/well) were seed into 6-well plates and added miR-223-3p knock out-containing mADSC-Exos and/or FUGW-miR-223-3p-GSG-P2A-EGFP or mADSC-Exos (10 µg/mL) for 48 hours, and then incubated with 500 mOsm/kg hyperosmotic growth media for another 24 hours. Following the treatment, the supernatants from the culture medium were collected specifically for the analysis of IL-6 levels.

Dual Luciferase Reporter Assays

The predicted miR-223-3p binding site of the Fbxw7 3′-UTR sequence (Position 235-242: 5′-agacaagagaccgu aacugacaggaggcgg-3′; Position 1176-1183: 5′-gaacauacauagc aaaacugacaagauauu-3′) or mutant sequence (Position 235-242: 5′- agacaagagaccguaugacucaggaggcgg-3′; Position 1176-1183: 5′-gaacauacau agcaaaugacucaagauauu-3′) was cloned into the pGL3-control firefly luciferase control vector (Promega, Madison, WI, USA) to construct the Fbxw7-3′-UTR-WT (wild-type) plasmid or the Fbxw7-3′-UTR-Mut (mutants) plasmid. MCECs cells (1×10^4 cells/well) were seeded into 96-well plates and were transiently transfected with 400 ng renilla luciferase-expressing plasmid (pRL-TK; Promega, Madison, WI, USA) and 1000 ng pGL3-Fbxw7-3′-UTR-WT luciferase reporter plasmid or the pGL3-Fbxw7-3′-UTR-Mut luciferase reporter plasmid according to the protocol of Lipofectamine 3000 transfection reagent (Thermo Fisher Scientific Inc., Waltham, MA, USA). The FUGW-miR-223-3p-GSG-P2A-EGFP or pGreenPuro siRNA-anti-miR-223-3p were co-added into MCECs cells for 48 hours. Following the treatment, MCECs were harvested for conducting

Investigative Ophthalmology & Visual Science

Table. Primer Sequences

Gens	Sense	Anti-Sense
IL-6	5′- TCTATACCACTTCACAAGTCGGA-3′	5′- GAATTGCCATTGCACAACTCTTT-3′
TNF-α	5′- CCCTCACACTCAGATCATCTTCT-3′	5′- GCTACGACGTGGGCTACAG-3′
IL-1β	5′- GTCGCTCAGGGTCACAAG-3′	5′- GTGCTGCCTAATGTCCCC-3′
Fbxw7	5′- ACCGCTTCTTCCTCAGTTCC-3′	5′- CTTCAGAGTCGAGCGGTGG-3′
MUC5AC	5′- TCTACTGACTGCACCAACACA-3′	5′- TCCGTCAGTCCACACTTTCG-3′
miR-223-3p	5′- GCCGAGTGTCAGTTTGTCAAAT-3′	5′- AGTGCAGGGTCCGAGGTATT-3′
U6 snRNA	5′- CTCGCTTCGGCAGCACA-3′	5′- AACGCTTCACGAATTTGCGT-3′
18S rRNA	5′- GTAACCCGTTGAACCCCATT-3′	5′- CCATCCAATCGGTAGTAGCG-3′
miR-223-3p RT primer	5′- GTCGTATCCAGTGCAGGGTCCGAGGTATTCGCACTGGATACGACTGGGGT-3′	
U6 snRNA RT primer	5′- AACGCTTCACGAATTTGCGT-3′	

dual luciferase reporter assays (Promega, Madison, WI, USA). Luciferase values were normalized to the internal control renilla.

Western Blot Analysis

Following the determination of protein concentration using the bicinchoninic acid (BCA) method, equal amounts of proteins were separated through 10% to 15% (w/v) SDS-PAGE. Subsequently, the proteins were transferred onto a polyvinyl difluoride (PVDF) membrane (Bio-Rad Laboratories, Inc., Hercules, CA, USA) at a current of 300 mA for 2 hours. Following a 2-hour blocking period at room temperature using 5% non-fat milk, the membranes were incubated with primary antibodies overnight at 4°C. Post-incubation with secondary antibodies, the reaction product on the membranes was visualized using a BeyoECL Plus detection kit. Western blot images and the densities of the bands were captured and quantitatively analyzed using the protein imaging system (Servicebio, Wuhan, China). The antibodies against IL-6 (#12912, 1:1000), TNF-α (#3707, 1:1000), IL-1β (#12242, 1:1000), and loading control β-actin (#8457, 1:2000) were purchased from Cell Signaling Technology (Danvers, MA, USA). The Fbxw7 antibody (ab192328, 1:1000) was purchased from Abcam (Waltham, MA, USA).

Quantitative Real-Time Fluorescence Polymerase Chain Reaction Assay

The quantitative real-time PCR (qRT-PCR) assay was performed using SYBR Green (Thermo Fisher Scientific Inc., Waltham, MA, USA) in an Agilent PCR System. The primers used for qRT-PCR detection are listed in the Table. The $2^{-\Delta\Delta Ct}$ rate was used to calculate the relative mRNA levels. U6 snRNA was used as an internal control for miR-223-3p. The 18S rRNA gene was used as an internal control for the other genes.

ELISA Assay

Corneal and conjunctival tissues from eyes were collected and extracted using cold RIPA buffer (Beyotime, Shanghai, China). Protein concentrations were measured with the BCA kit (Beyotime, Shanghai, China). Levels of IL-6, IL-1β, and TNF-α (all measured in pg/mL) in cell supernatants, as well as levels of IL-6, IL-1β, and TNF-α (all measured in pg/mg) in corneal and conjunctival tissues, were meticulously measured according to the protocols provided by Ruixin Biotechnology Co., Ltd. (Quanzhou, China) and Hangzhou Lianke Biotechnology Co., Ltd. (Hangzhou, China), respectively. Levels of IL-17, C-C Motif Chemokine Ligand 2 (CCL2), and C-X-C Motif Chemokine Ligand 1 (CXCL1; all in pg/mg protein) were determined according to the manufacturer's instructions using the ELISA Kit (Jiangsu Meimian Industrial Co., Ltd., Nantong, China).

Statistical Analysis

Data analysis was performed using GraphPad Prism version 10.0 software (San Diego, CA, USA). The data were presented as mean ± standard deviation (SD). A P value less than 0.05 was considered to indicate statistical significance. For comparisons involving multiple groups, either 1-way or 2-way analysis of variance (ANOVA) was applied, followed by Tukey's or Dunnett's multiple comparison tests if the data were normally distributed and variances were similar, as confirmed by an F test ($P > 0.05$). In cases where variances differed (F test, $P < 0.05$), the Brown-Forsythe and Welch ANOVA tests were utilized. If the data did not conform to a normal distribution, the Kruskal-Wallis test followed by Dunn's multiple comparisons test was used.

Results

miR-223-3p May be an Important Active Molecule for mADSC-Exos Anti-Dry Eye Therapy

In our previous study, we presented compelling evidence that mADSC-Exos facilitated the repair of ocular surface epithelium and inhibited the production of inflammatory cytokines.[12] However, the key active molecules in mADSC-Exos that contribute to anti-dry eye therapy remain unclear. To further clarify whether miR-223-3p is the crucial active molecule for mADSC-Exos anti-dry eye therapy. Initially, we evaluated the expression of miR-223-3p mRNA in mADSC, mADSC-Exos, and MCECs. As shown in Figure 1A, the results indicated a significant increase in miR-223-3p mRNA content in mADSC-Exos compared to MECS cells. Next, we analysed the levels of miR-223-3p mRNA in a mouse dry eye model induced by BAC. As illustrated in Figure 1B, the model group exhibited a significant decrease in miR-223-3p mRNA levels. In contrast, the administration of mADSC-Exos resulted in a dose-dependent increase in miR-223-3p mRNA. Similarly, in the hyperosmotic-induced MCECs model, a decrease in miR-223-3p mRNA content was observed in the model group. However, the expression of miR-223-3p mRNA was increased with the introduction of mADSC-Exos (Fig. 1C). Before measuring the effect of miR-223-3p overexpression

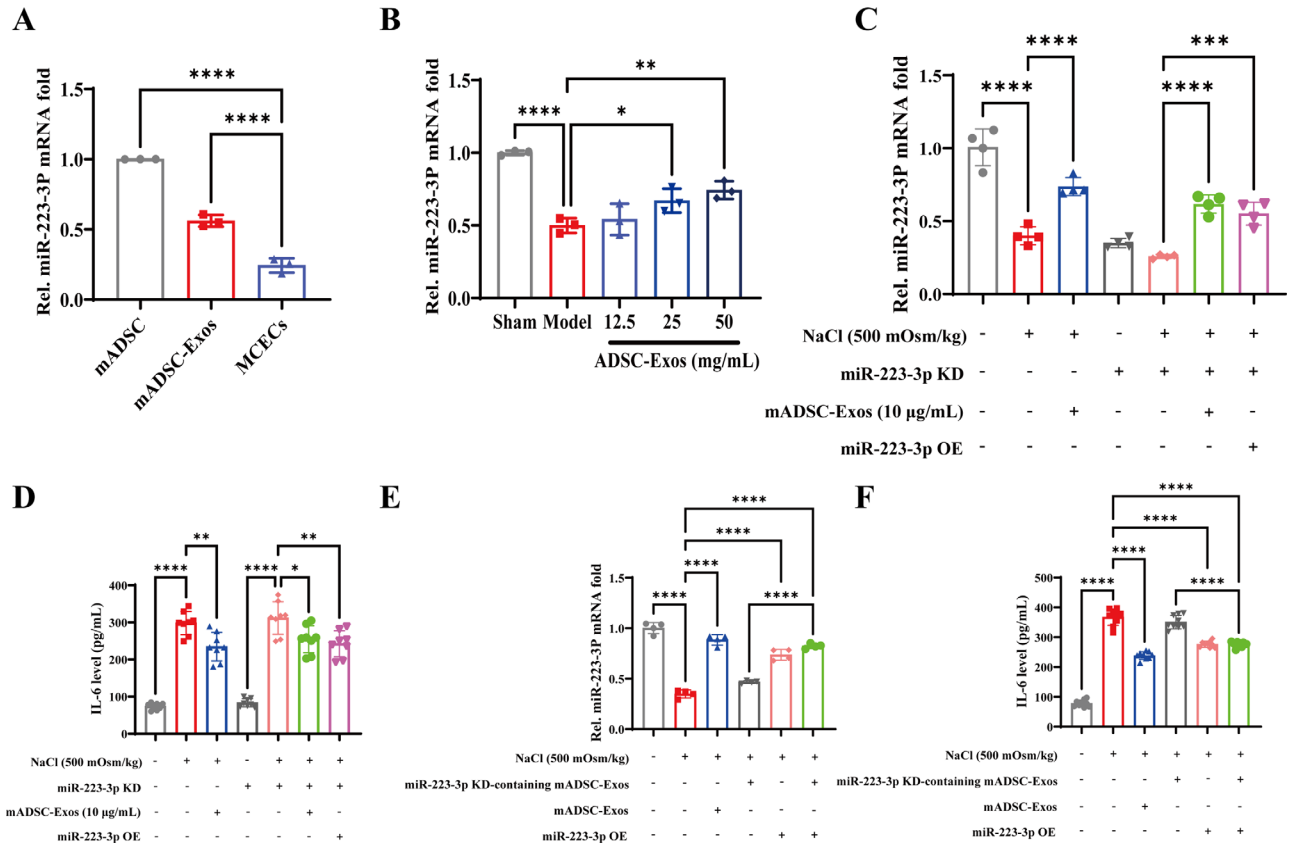

Figure 1. The miR-223-3p may be an important active molecule of mADSC-Exos. (**A**) mRNA levels of miR-223-3p in mADSC, mADSC-Exos, and MCECs. (**B**) Comparative mRNA levels of miR-223-3p in the cornea and conjunctiva tissues. (**C**, **E**) Examination of mRNA levels of miR-223-3p in MCECs subjected to hyperosmolar conditions. (**D**, **F**) IL-6 levels in hyperosmolarity-induced MCECs. Data were analyzed using ordinary 1-way ANOVA followed by Dunnett's multiple comparisons test (**A**, **B**) or Tukey's multiple comparisons test (**C–F**). $^{*}P < 0.05$, $^{**}P < 0.01$, $^{***}P < 0.001$, and $^{****}P < 0.0001$.

or knockdown on IL-6 levels, it is necessary to demonstrate the impact of miR-223-3p overexpression or knockdown on cell viability. The results of the CCK-8 assay showed that there was no significant difference in cell viability due to miR-223-3p overexpression or knockdown (Supplementary Fig. S1). After silencing miR-223-3p in hyperosmotic-induced MCECs cells, subsequent treatment with mADSC-Exos resulted in the overexpression of miR-223-3p, which significantly reduced the increase in IL-6 content induced by hyperosmotic conditions (Fig. 1D). Crucially, when mADSC-Exos, in which miR-223-3p had been knocked out, were added to the hyperosmotic-induced MCECs cell model, there was no increase in mRNA expression of miR-223-3p (Fig. 1E). Additionally, mADSC-Exos without miR-223-3p did not reduce IL-6 content. However, subsequent treatment with mADSC-Exos or overexpression of miR-223-3p significantly reduced the IL-6 content (Fig. 1F). In summary, miR-223-3p could be a significant active molecule in the treatment of dry eye disease with mADSC-Exos.

miR-223-3p Alleviated Tear Film Stability and Corneal Surface Damage in Both BAC- and Scop-Induced Mouse Models

To assess the therapeutic efficacy of miR-223-3p in dry eye, we used a lentiviral vector-mediated overexpression strategy in both BAC- and Scop-induced mouse models (Fig. 2A, Supplementary Fig. S3A). Although body and eyeball weights remained comparable across groups (Supplementary Figs. S2A, S2B, S3B), fluorescein staining scores were significantly elevated in both dry eye models compared to sham controls, indicating exacerbated corneal damage. Notably, miR-223-3p overexpression significantly reduced fluorescein staining scores, suggesting a protective effect on corneal integrity (see Figs. 2B, 2C, Supplementary Figs. S3C, S3D). Furthermore, both tear volume and BUT were significantly reduced in dry eye models compared to sham controls (see Figs. 2D, 2E, Supplementary Figs. S3E, S3F). However, miR-223-3p treatment significantly improved these parameters, demonstrating a superior therapeutic effect compared to pranoprofen. Collectively, these findings highlight the therapeutic potential of miR-223-3p in alleviating both BAC- and Scop-induced dry eye in mice.

miR-223-3p Suppressed the Histopathological Changes in Corneal and Conjunctival Tissues in a BAC-Induced Dry Eye Mouse Model

Histological examination of the corneal and conjunctival tissue was conducted using H&E staining. As shown in Figures 3A and 3B, the model group exhibited greater infiltration of inflammatory cells in the central cornea and conjunctiva region compared to the miR-223-3p overexpression group and sham group. In addition, miR-223-3p over-

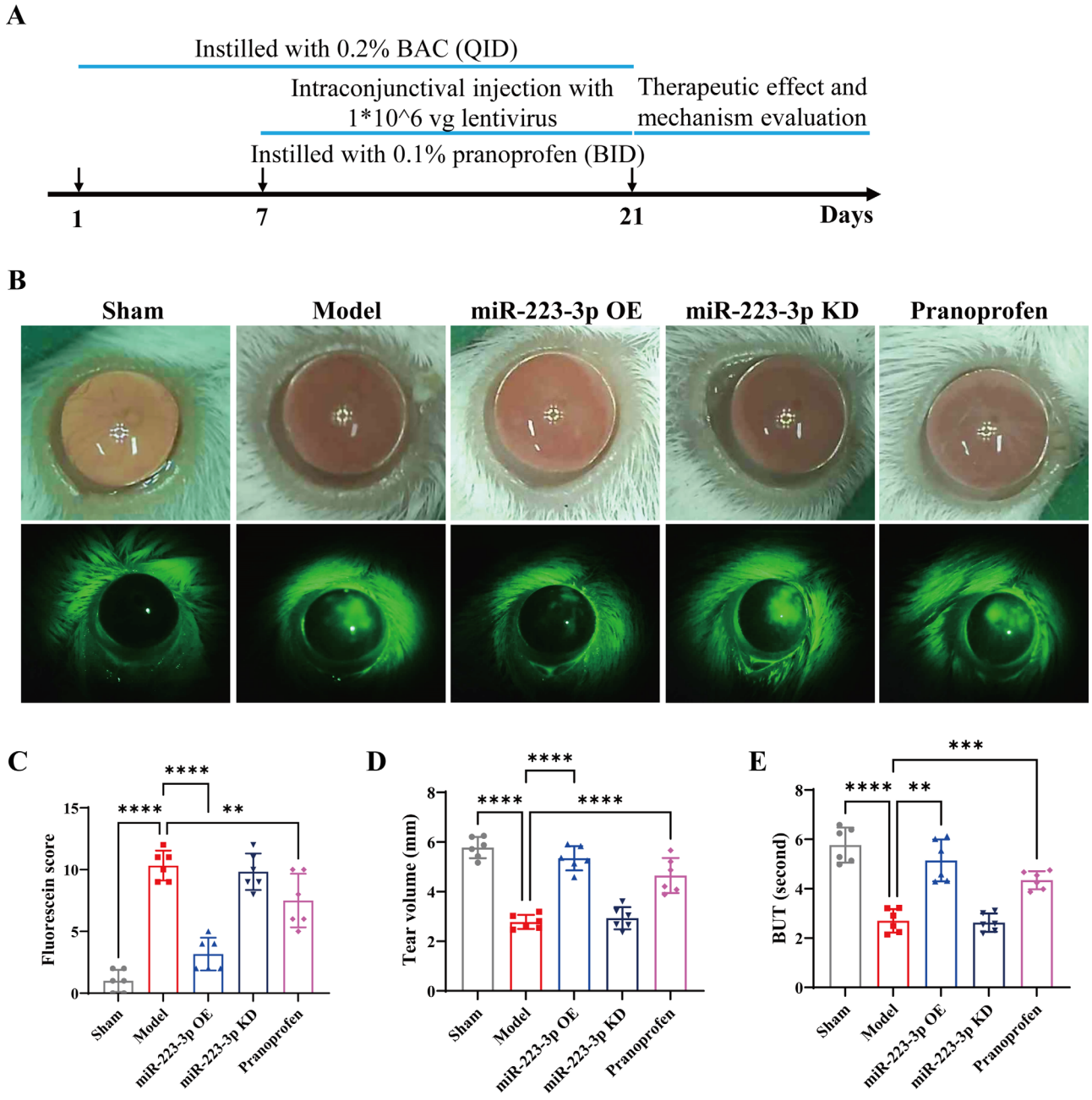

Figure 2. The miR-223-3p improved dry eye symptoms in BAC-induced mouse dry eye model. (**A**) Diagram of the experiment schedule. (**B**) Representative corneal fluorescein staining images. (**C**) Fluorescein staining score. (**D**) Tear volume (mm). (**E**) BUT (s). Data were analyzed using ordinary 1-way (**C**, **D**) or Brown-Forsythe and Welch ANOVA multiple comparisons test (**E**). $^{**}P < 0.01$, $^{***}P < 0.001$, and $^{****}P < 0.0001$ versus model group. BID = twice daily and QID = 4 times a day.

expression reversed the corneal and conjunctiva epithelial thickness (Figs. 3C–3E). The results suggest that miR-223-3p suppressed the histopathological damage induced by BAC.

miR-223-3p Increased the Number of Goblet Cells and Inhibited Conjunctival Epithelial Cells Apoptosis in BAC-Induced Mouse Dry Eye Model

The conjunctival epithelium, characterized by superficially scattered goblet cells responsible for producing mucins essential for the tear film, was examined. Periodic acid Schiff (PAS) staining (Fig. 4A) showed that conjunctival goblet cell density was significantly increased after the treatment with miR-223-3p (Fig. 4B). The miR-223-3p increased the murine fornix conjunctival goblet cell-specific mucin MUC5AC expression in the BAC-induced mouse dry eye model, suggesting that miR-223-3p overexpression can reduce the loss of conjunctival epithelial goblet cells (Figs. 4C–4E). Following this, we identified apoptotic cells in the conjunctival tissue through the TUNEL assay. There was a notable increase in the number of TUNEL-positive cells in the model group when compared to the sham group.

Investigative Ophthalmology & Visual Science

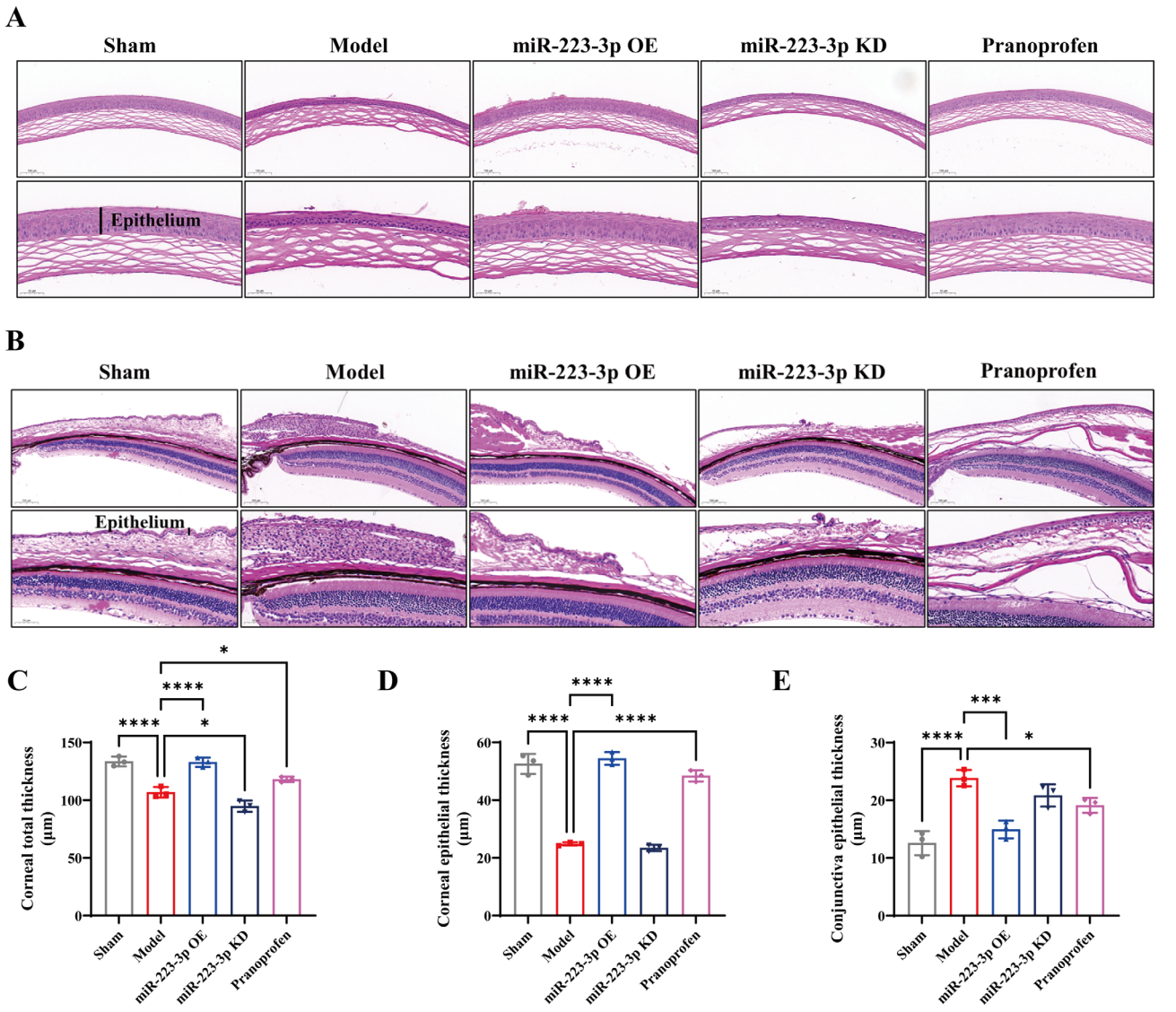

Figure 3. Effects of miR-223-3p on histopathological of corneal and conjunctival tissues. (**A**) Representative H&E staining images of corneal. Scale bar = 50 µm and 100 µm. (**B**) Representative H&E staining images of conjunctiva. Scale bar = 50 µm and 100 µm. (**C**) Corneal total thickness (µm). (**D**) Corneal epithelial thickness (µm). (**E**) Conjunctiva epithelial thickness (µm). Data were analyzed using ordinary 1-way ANOVA followed by Dunnett's multiple comparisons test (**C–E**). *$P < 0.05$, ***$P < 0.001$, and ****$P < 0.0001$.

Conversely, treatment with miR-223-3p resulted in a reduction in the number of apoptotic cells (Figs. 4F, 4G). Collectively, these findings demonstrate that miR-223-3p treatment effectively enhances goblet cell density in a BAC-induced dry eye mouse model.

miR-223-3p Suppressed the Inflammatory Response in Both BAC- and Scop-Induced Mouse Models

Dry eye severity is frequently linked to elevated levels of pro-inflammatory cytokines. The impact of miR-223-3p on pro-inflammatory cytokine production in corneal and conjunctival tissues of BAC- and Scop-induced mouse dry eye model was further examined. Compared to the control group, the expressions of IL-6, TNF-α, and IL-1β proteins were significantly higher in both dry eye models (Figs. 5A–5D and Supplementary Figs. S3G–S3I). Likewise, there was a significant increase in the mRNA levels of these pro-inflammatory cytokines and CCL-2, IL-17, and CXCL-1 levels in the model group (Figs. 5E–5J). However, miR-223-3p effectively reduced the levels of these pro-inflammatory cytokines in the corneal and conjunctival tissues, outperforming the positive control treatment (0.1% pranoprofen). These findings indicate that miR-223-3p could be a potential therapeutic option for treating dry eye by suppressing the inflammatory response.

miR-223-3p Regulated Fbxw7 Expression

To identify the target protein influenced by miR-223-3p, we initially predicted the target genes of miR-223-3p using TargetScan7.1, miRbase, and miRDB, using a highly stringent enrichment analysis, and a total of 16 target genes were predicted. Among these, only Fbxw7, Stat3, Foxo3, and Foxo1 were shown to be associated with the inflammation response. As illustrated in Figures 6A to 6C, miR-

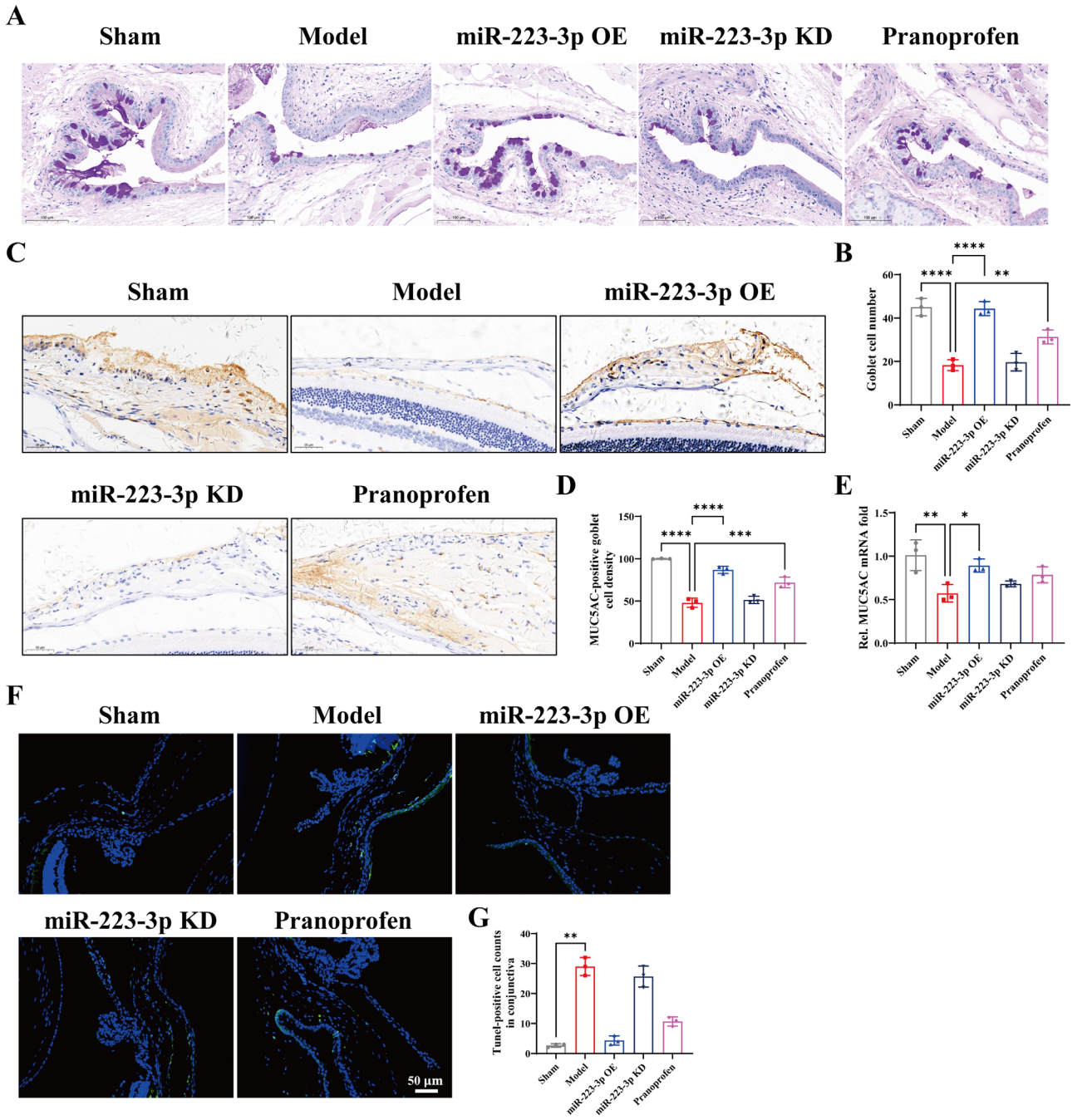

Figure 4. The miR-223-3p increased the number of goblet cells and inhibited conjunctival epithelial cells apoptosis. (**A**) Representative PAS staining of conjunctival goblet cells. Scale bar = 100 μm. (**B**) Goblet cell number. (**C**) Immunohistochemistry for MUC5AC in the conjunctiva. Scale bar = 50 μm. (**D**) MUC5AC-positive goblet cell density. (**E**) The mRNA levels of MUC5AC. (**F**) Representative images display TUNEL staining (in *green*) identifying apoptotic cells, along with DAPI staining (in *blue*) marking the nuclei in the conjunctiva. Scale bars = 50 μm. (**G**) Quantification of TUNEL-positive cells. Data were analyzed using ordinary 1-way ANOVA followed by Dunnett's multiple comparisons test (**B, D,** and **E**) or Kruskal-Wallis test followed by Dunn's multiple comparisons test (**G**). $^{*}P < 0.05$, $^{**}P < 0.01$, $^{***}P < 0.001$, and $^{****}P < 0.0001$.

223-3p significantly decreased the levels of Fbxw7 in the corneal and conjunctival tissues. Similarly, in comparison to the control cells, FUGW-miR-223-3p significantly reduced the expression of Fbxw7 protein in MCECs cells (Fig. 6D). Conversely, the pGreenPuro siRNA-anti-miR-223-3p significantly increased the expression of Fbxw7 protein in MCECs cells (Fig. 6E). These results indicate that Fbxw7 is the specific target of miR-223-3p.

Fbxw7 Knockdown Suppressed Inflammation in Hyperosmolarity-Induced MCECs

To further investigate whether blocking Fbxw7 expression has a similar anti-inflammatory effect to that of miR-223-3p in hyperosmolarity-induced MCECs, we first detected the protein expression using the constructed Fbxw7 overexpression or knockdown plasmid (Figs. 7A, 7B). The efficacy of

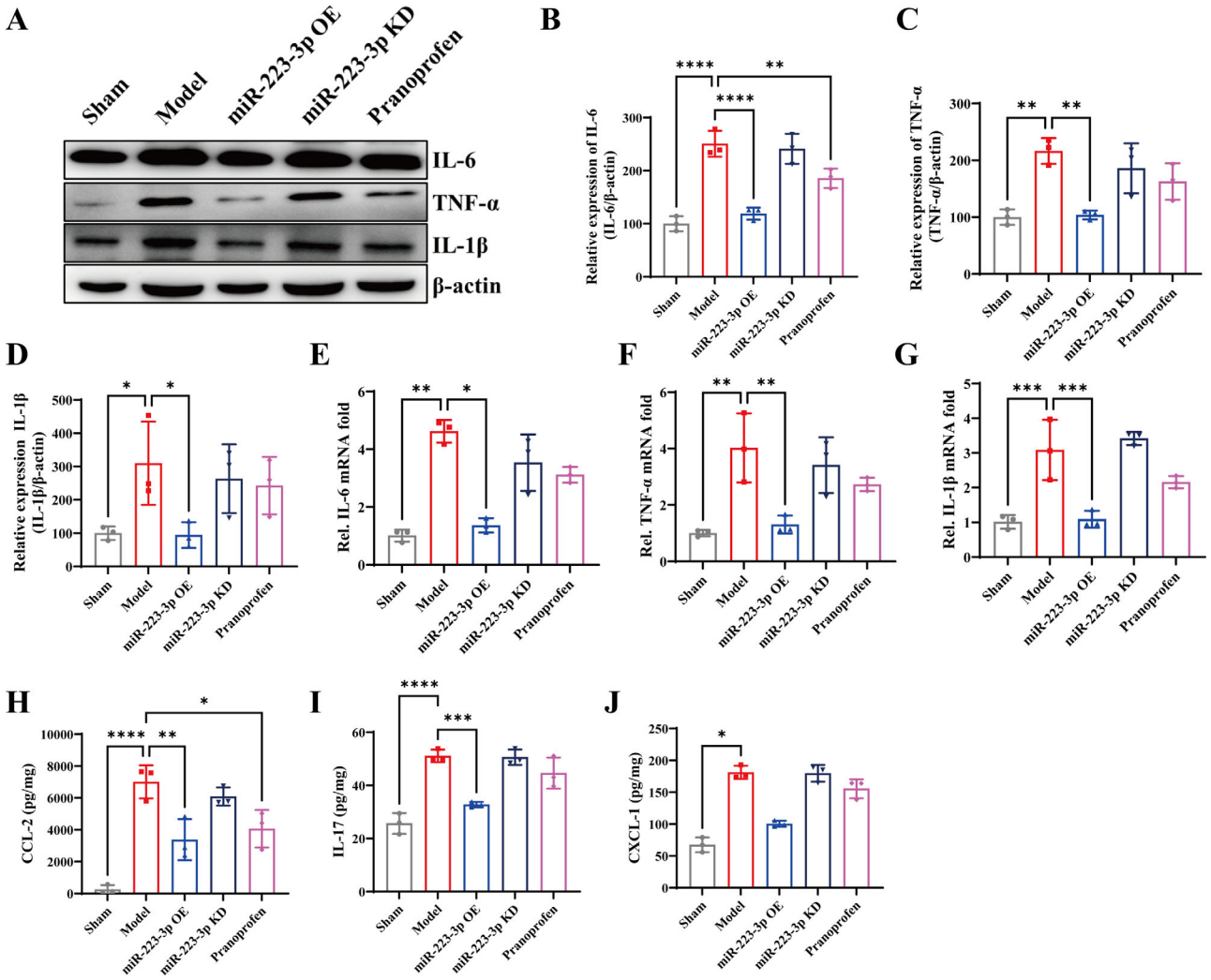

Figure 5. Effects of miR-223-3p on the production of pro-inflammatory cytokines. (**A–D**) Western blotting and quantitative analysis of IL-6, TNF-α, and IL-1β. (**E–G**) mRNA levels of IL-6, TNF-α, and IL-1β in corneal and conjunctival tissues were determined using qRT-PCR. (**H–J**) CCL-2, IL-17, and CXCL-1 levels (pg/mg protein). The data were subjected to analysis using ordinary 1-way ANOVA and Dunnett's multiple comparisons test (**B–D, F–J**), or Kruskal-Wallis test followed by Dunn's multiple comparisons test (**E**). *$P < 0.05$, **$P < 0.01$, ***$P < 0.001$, and ****$P < 0.001$ versus the model group.

these plasmids in modulating Fbxw7 expression was verified through Western blot analysis. Subsequently, MCECs were subjected to hyperosmotic stress in the presence of either Fbxw7 overexpression or knockdown constructs, to evaluate their impact on IL-6, TNF-α, and IL-1β content and compare it with the effects observed under miR-223-3p modulation. As shown in Figures 7C to 7E, Fbxw7 shRNA suppressed the inflammatory effect. The results indicated that miR-223-3p may suppress hyperosmolarity-induced inflammation by blocking the expression of Fbxw7.

miR-223-3p Suppressed the 3′-UTR Regions of Fbxw7

The targeting of the Fbxw7 gene silencing region by miR-223-3p was evaluated using dual luciferase gene reporter assays. TargetScanMouse (https://www.targetscan.org/mmu_80/) predicted that miR-223-3p binds to bases 235 to 242 and 1176 to 1183 of the 3′-untranslated region (3′-UTR) of Fbxw7 mRNA (Fig. 8A). The miR-223-3p was found to decrease the luciferase activity of the plasmid that contained the WT fragment of the Fbxw7 3′-UTR. In contrast, the luciferase activity of the plasmid with the mutated Fbxw7 3′-UTR fragment remained unaffected by both the miR-223-3p mimics and the negative control. These results suggested that miR-223-3p could bind to the 3′-UTR regions of Fbxw7 mRNA (Fig. 8B).

Discussion

Current clinical treatments for dry eye predominantly focus on providing symptomatic relief. However, a significant limitation of these therapies is their delayed effectiveness. In contrast, although rapid anti-inflammatory drugs are available, their use is often marred by considerable side effects, posing a dilemma in the management of this condition. Recent research has highlighted the role of miRNA alterations in dry eye syndrome, opening new avenues for treatment.[19–22] Studies have found that miR-223-3p is a key regu-

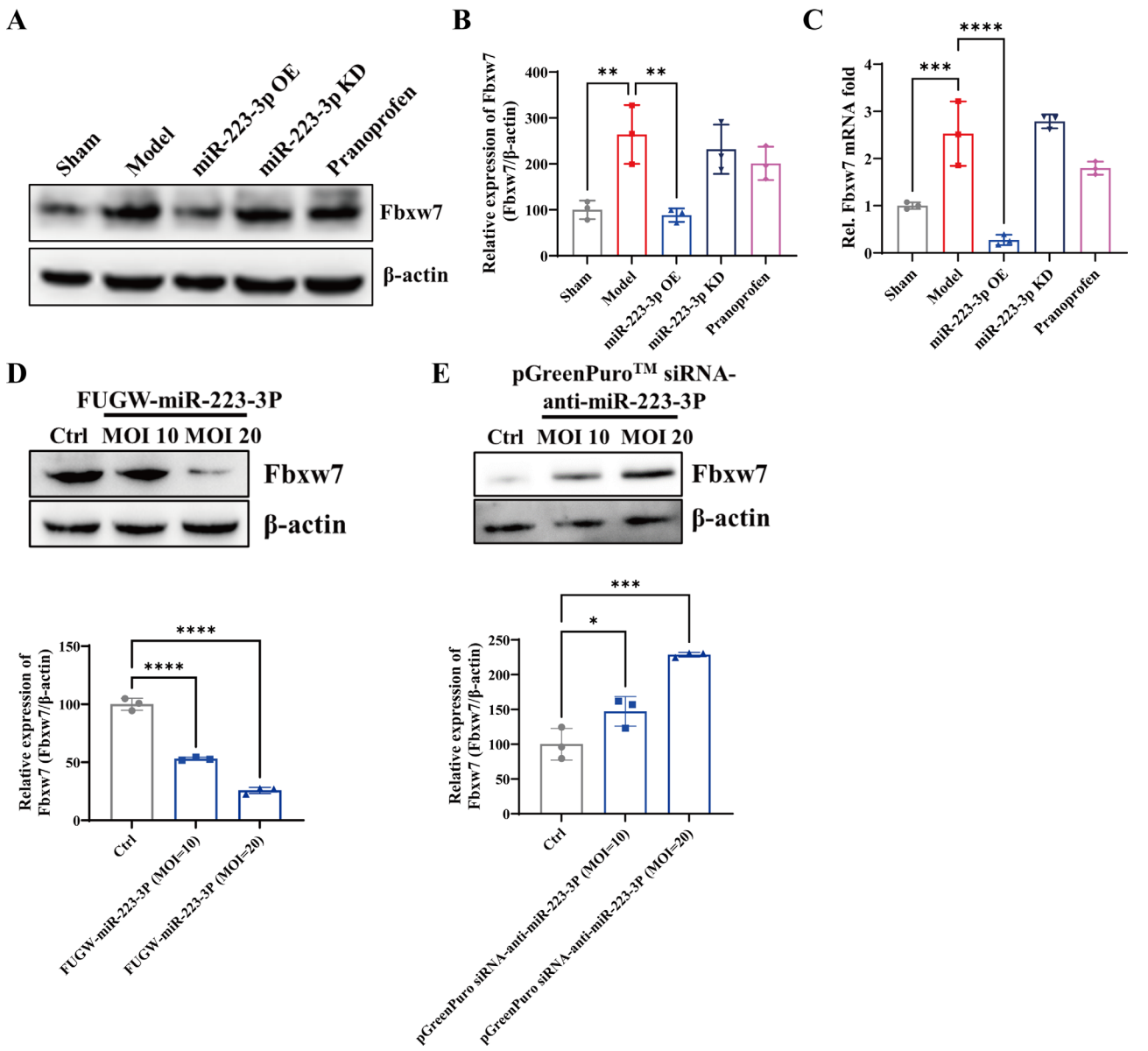

Figure 6. Fbxw7 was the direct target of miR-223-3p. (**A**, **B**) Western blotting and quantitative analysis of Fbxw7 in corneal and conjunctival tissues. (**C**) The mRNA levels of Fbxw7 in corneal and conjunctival tissues. (**D, E**) Western blotting and quantitative analysis of Fbxw7 in MCECs. The data were subjected to analysis using ordinary 1-way ANOVA and Dunnett's multiple comparisons test. *$P < 0.05$, **$P < 0.01$, ***$P < 0.001$, and ****$P < 0.0001$.

lator for the inflammatory response in various diseases.[13–15] However, its therapeutic potential and underlying mechanisms in dry eye remain largely unexplored. Our research revealed a significant decrease in miR-223-3p levels in both streptozotocin-induced diabetic keratopathy (data not shown) and BAC-induced dry eye mouse models, suggesting its potential therapeutic role. We further demonstrated that miR-223-3p effectively attenuates ocular surface damage and inhibits the inflammatory response in dry eye mouse models. These findings highlight the clinical significance of miR-223-3p in dry eye syndrome and provide novel insights into potential therapeutic strategies. This discovery paves the way for novel treatment strategies for dry eye syndrome, especially in cases where conventional therapies fall short.

Animal models mimicking human dry eye disease are crucial tools for understanding its pathophysiology and evaluating the therapeutic efficacy of new treatments. Over the years, several animal models have been developed based on various etiologies of dry eye, including evaporative models, meibomian gland dysfunction models, dacryoadenectomy, induced autoimmune dacryoadenitis, drainage duct injury models, and topical application of BAC.[23] Whereas these models have shown promising results, each has limitations and cannot fully replicate the pathophysiological mechanisms occurring in patients. Nevertheless, for the purposes of this study, we selected the BAC-induced and Scop-induced mouse dry eye models, which serve as representative models for quantitative (aqueous-deficient) and qualitative (evaporative) dry eye, respectively.[18,24–26] Future studies should incorporate a wider range of models to comprehensively understand the therapeutic potential of mADSC-derived exosomal miR-223-3p in dry eye disease and enhance its

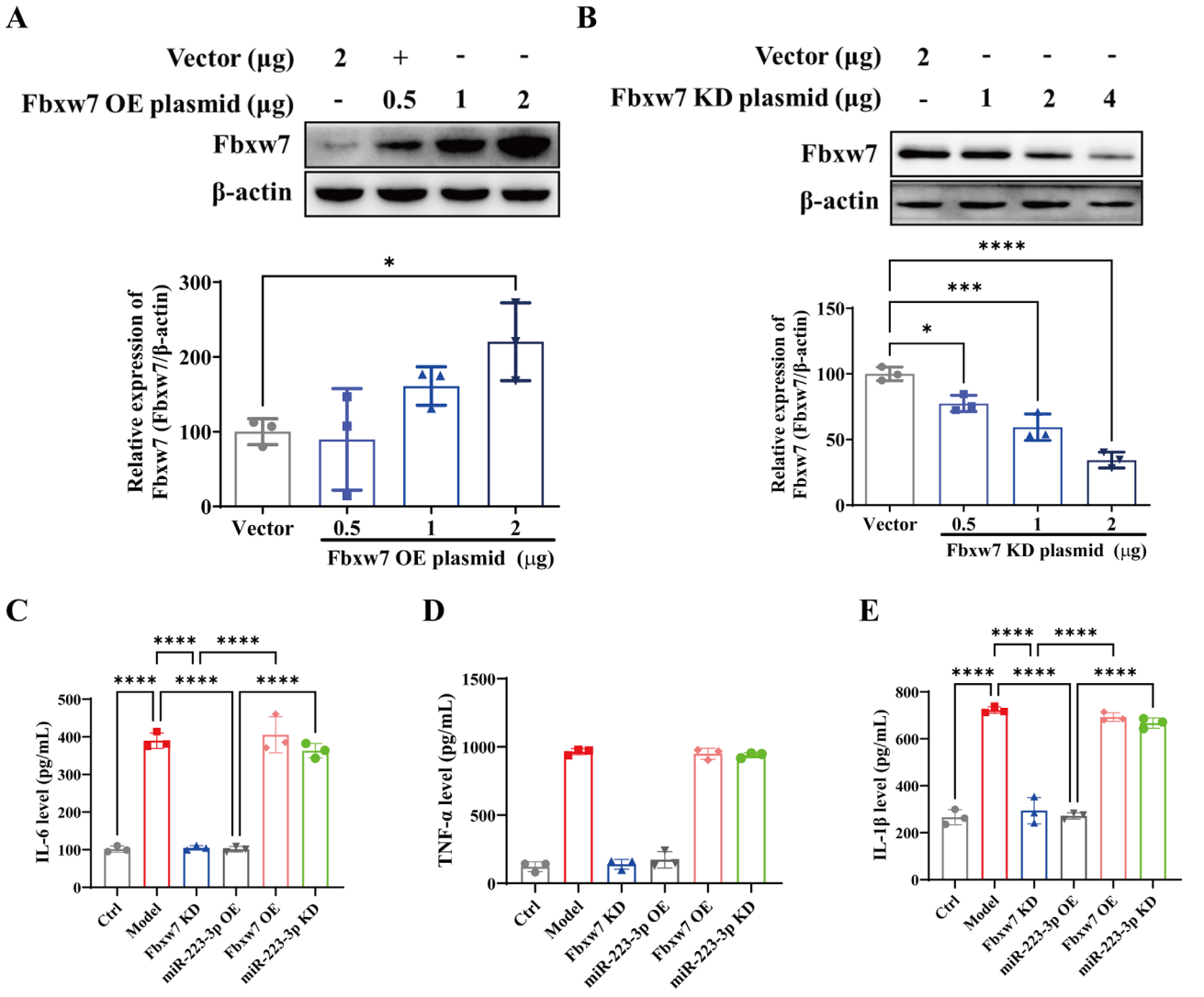

Figure 7. Fbxw7 knockdown suppressed inflammation in hyperosmolarity-induced MCECs. (**A**, **B**) Western blotting and quantitative analysis of Fbxw7 in MCECs. (**C–E**) Downregulation of Fbxw7 by specific shRNA reduced IL-6 (**C**), TNF-α (**D**), and IL-1β (**E**) levels in hyperosmolarity-induced MCECs. Data were analyzed using 1-way ANOVA and Tukey's multiple comparison tests. *$P < 0.05$, ***$P < 0.001$, and ****$P < 0.0001$.

translational relevance. Despite inherent limitations, this study offers valuable insights and charts a course for future research endeavors. In line with previous studies, we identified significant ocular surface damage and elevated levels of pro-inflammatory cytokines (IL-1β, IL-6, IL-17, and TNF-α) and chemokines (CCL2 and CXCL1) in BAC-induced mice, underscoring the pivotal role of inflammation in dry eye pathogenesis.[27] Our TUNEL assay results also revealed increased apoptosis of conjunctival epithelial cells in the dry eye group, aligning with prior research findings.[28] Furthermore, we confirmed ocular surface damage in Scop-induced mice, consistent with earlier findings.[25,26] Previous research has linked miR-223-3p to vascular endothelial injury, synaptic function, inflammatory response, and other mechanisms.[29] Li et al.[30] demonstrated that overexpression of miR-223-3p inhibited the secretion of IL-1β and IL-18 by regulating the NLRP3/caspase-1 pathway in mice. Wan et al.[31] also found that miR-223-3p regulates NLRP3, promoting apoptosis and inhibiting proliferation of hep3B cells. Compared to the control group, the expression level of miR-223-3p was significantly decreased in the conjunctiva and cornea of dry eye mice and patients with dry eye, whereas the expression levels of NLRP3 and IL-1β increased.[32] Interestingly, treatment with miR-223-3p effectively repaired ocular surface damage, inhibited cell apoptosis, and reduced pro-inflammatory cytokines in the BAC-induced dry eye model. Moreover, miR-223-3p significantly improved ocular surface damage in Scop-induced mice, highlighting its potential therapeutic efficacy in both evaporative and aqueous-deficient dry eye models. Given that inflammation is a central feature of both dry eye models, we propose that miR-223-3p may exert its therapeutic effects by modulating the expression of specific genes or regulatory pathways involved in controlling inflammatory responses. Further research should explore these mechanisms to fully elucidate the therapeutic potential of miR-223-3p in dry eye treatment. Although Yu Jeong Kim et al.[17] found that miR-223-3p expression was higher in patients with Sjögren syndrome compared to the control group. We speculated that this discrepancy may arise from the fact that their samples were taken from sera or salivary glands, or due to the distinct nature of Sjögren syndrome compared to

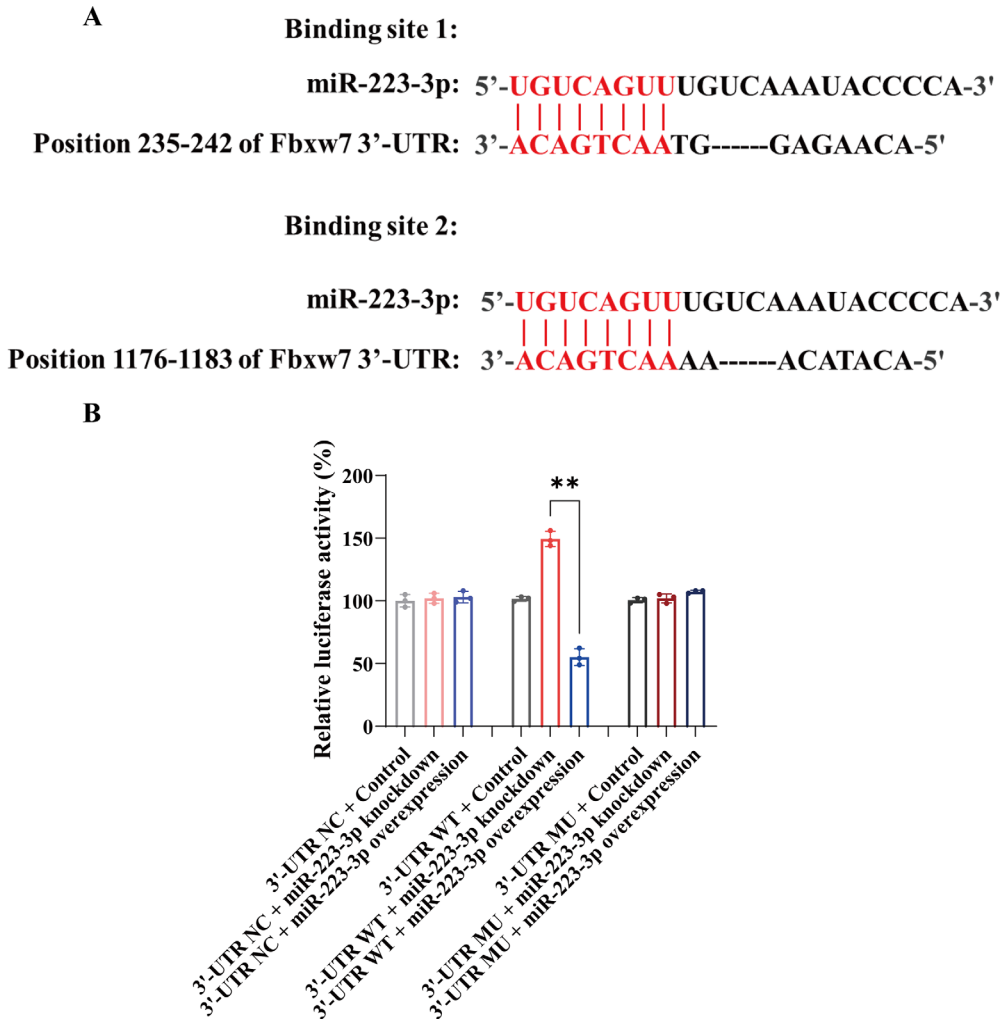

Figure 8. The miR-223-3p can bind to the 3′-UTR region and regulate Fbxw7 expression. (**A**) Predicted potential binding sites of miR-223-3p and Fbxw7 mRNA are displayed in the *upper panel*. (**B**) Relative luciferase activity (%). For analysis, 2-way ANOVA and Tukey's multiple comparisons test were utilized. $^{**}P < 0.01$.

dry eye disease. Moreover, miR-223-3p holds potential as an early diagnostic biomarker for dry eye syndrome. By detecting specific miR-223-3p levels in tear fluid, serum, or corneal tissue, early diagnosis can be achieved. Additionally, miR-223-3p could be used alongside existing treatments for dry eye, such as artificial tears and anti-inflammatory drugs, to enhance efficacy and reduce side effects. Based on the miRNA expression profile of the patient, personalized treatment plans can be formulated to optimize therapeutic outcomes.

Fbxw7, functioning as an E3 ubiquitin ligase, plays a crucial role in various regulatory processes, including cell survival, cell proliferation, tumor invasion, DNA damage repair, lipid metabolism, and targeting osteogenic and chondrogenic transcription factors. Additionally, Fbxw7 is involved in maintaining genome stability and influencing telomere biology.[33,34] Modulating proteasome-mediated degradation of TRAF6 in cells can target the inhibition of Sjögren syndrome-like autoimmunity and BAFF-induced B cell hyperactivation.[35] He et al.[36] found that Fbxw7 deficiency increased CCL2/7 in CX3CR1hi macrophages, which protected mice from intestinal inflammation induced by dextran sodium sulfate and 2,6,4-trinitrobenzene sulfonic acid. Zhang et al.[37] found that miR-223-3p could inhibit the expression of Fbxw7, leading to a reduction in inflammatory response and apoptosis in both H9c2 cells and cardiac tissues. The overexpression of Fbxw7 promoted HG-induced endothelial dysfunction, including apoptosis, abnormal vascular differentiation, and secretion of inflammatory factors.[38] However, another study has revealed that Fbxw7α diminishes inflammatory signaling in primary macrophages by reducing the levels of C/EBPδ and its target gene, Toll-like receptor 4 (TLR4).[39] The Fbxw7 overexpression was found to enhance the recovery from septic liver injury induced by lipopolysaccharide (LPS) through the suppression of apoptosis, inflammation, and oxidative reactions.[40] In our study, Fbxw7 is one of the direct target genes regulated by miR-223-3p, as predicted by the TargetScan, miRDB, and miRTarbase databases. The luciferase reporter assay results indicate that miR-223-3p directly targets Fbxw7 in MCECs. More importantly, Fbxw7 knockdown could reduce the contents of IL-1β, IL-6, and TNF-α. These results highlighted that miR-223-3p may suppress the inflammatory response in dry eye syndrome by blocking the expression of Fbxw7. Although the specific role and mechanisms of Fbxw7 in the inflammatory response associ-

ated with dry eye remain unclear, the study revealed that Fbxw7 enhances the ubiquitination of enhancer of zeste homolog 2 (EZH2). It has been demonstrated that a deficiency in EZH2 can impact TNF-α signaling and exacerbate the inflammatory response in intestinal epithelial cells.[41] We speculated that miR-223-3p may inhibit EZH2 degradation by targeting the inhibition of Fbxw7 expression, which in turn inhibits the inflammatory response in dry eye models.

Despite these promising findings, our study has several limitations. First, we confirmed the expression levels of miR-223-3p only in mouse samples. Future studies involving clinical samples should utilize qRT-PCR and miRNA sequencing to determine miR-223-3p expression levels for a more comprehensive understanding. Second, we examined the function of mADSC-Exos with miR-223-3p knockdown exclusively in vitro; in vivo experiments are necessary to further elucidate the role of miR-223-3p in mADSC-Exos, which may provide deeper insights into its impact on dry eye syndrome. Additionally, whereas we have preliminarily demonstrated the efficacy of miR-223-3p in both BAC-induced and Scop-induced mouse models of dry eye, the potential influence of other miRNAs present in mADSC-Exos cannot be entirely ruled out. The miRNAs typically target multiple genes, suggesting that miR-223-3p's effects on dry eye syndrome might involve various pathways beyond Fbxw7. Furthermore, the downstream signaling pathways resulting from the interaction between miR-223-3p and Fbxw7 remain unexplored. Future research should focus on delineating these pathways to fully understand their clinical implications.

Conclusions

In conclusion, the current study has demonstrated that miR-223-3p effectively inhibits inflammation in BAC- and Scop-induced mouse models of dry eye. To gain a deeper insight into the pathophysiology of dry eye, further research involving a larger sample size and a comprehensive exploration of the predicted molecular pathways is essential. Such studies are expected to provide a more robust experimental foundation for the clinical treatment of dry eye syndrome.

Acknowledgments

Supported by the Natural Science Foundation of Hunan Province (grant number 2023JJ30493), the Natural Science Foundation of Hunan Province (grant number 2020JJ5460), and Loudi Science and Technology Bureau (grant number [2022] No. 2).

Author Contributions: Guifang Wang designed and performed the experiments and analyzed the data. Yujie Zhu directed the project and wrote the manuscript. Yuzhen liu performed the qRT-PCR and immunohistochemistry staining studies. Mulin Yang performed the mice experiments. Li Zeng designed the cell experiments and analyzed the data. All authors have read and approved the final manuscript.

Data Availability Statements: All data generated or analyzed during this study are included in this article. Further enquiries can be directed to the corresponding author.

Disclosure: **G. Wang**, None; **Y. Zhu**, None; **Y. Liu**, None; **M. Yang**, None; **L. Zeng**, None

References

1. O'Neil EC, Henderson M, Massaro-Giordano M, Bunya VY. Advances in dry eye disease treatment. *Curr Opin Ophthalmol.* 2019;30:166–178.
2. Şimşek C, Doğru M, Kojima T, Tsubota K. Current management and treatment of dry eye disease. *Turk J Ophthalmol.* 2018;48:309–313.
3. Chang YA, Wu YY, Lin CT, et al. Animal models of dry eye: their strengths and limitations for studying human dry eye disease. *J Chin Med Assoc.* 2021;84:459–464.
4. Perez VL, Stern ME, Pflugfelder SC. Inflammatory basis for dry eye disease flares. *Exp Eye Res.* 2020;201:108294.
5. Periman LM, Perez VL, Saban DR, Lin MC, Neri P. The immunological basis of dry eye disease and current topical treatment options. *J Ocul Pharmacol Ther.* 2020;36:137–146.
6. Markoulli M, Hui A. Emerging targets of inflammation and tear secretion in dry eye disease. *Drug Discov Today.* 2019;24:1427–1432.
7. Zeng J, Wu M, Zhou Y, Zhu M, Liu X. Neutrophil extracellular traps (NETs) in ocular diseases: an update. *Biomolecules.* 2022;12:1440.
8. An S, Raju I, Surenkhuu B, et al. Neutrophil extracellular traps (NETs) contribute to pathological changes of ocular graft-vs.-host disease (oGVHD) dry eye: implications for novel biomarkers and therapeutic strategies. *Ocul Surf.* 2019;17:589–614.
9. Rassi DM, De Paiva CS, Dias LC, et al. Review: MicroRNAS in ocular surface and dry eye diseases. *Ocul Surf.* 2017;15:660–669.
10. Liao CH, Tseng CL, Lin SL, Liang CL, Juo SH. MicroRNA therapy for dry eye disease. *J Ocul Pharmacol Ther.* 2022;38:125–132.
11. Yin L, Zhang M, He T, Chen S. The expression of miRNA-146a-5p and its mechanism of treating dry eye syndrome. *J Clin Lab Anal.* 2021;35:e23571.
12. Wang G, Li H, Long H, Gong X, Hu S, Gong C. Exosomes derived from mouse adipose-derived mesenchymal stem cells alleviate benzalkonium chloride-induced mouse dry eye model via inhibiting NLRP3 inflammasome. *Ophthalmic Res.* 2022;65:40–51.
13. Houshmandfar S, Saeedi-Boroujeni A, Rashno M, Khodadadi A, Mahmoudian-Sani MR. miRNA-223 as a regulator of inflammation and NLRP3 inflammasome, the main fragments in the puzzle of immunopathogenesis of different inflammatory diseases and COVID-19. *Naunyn Schmiedebergs Arch Pharmacol.* 2021;394:2187–2195.
14. Shi X, Xie X, Sun Y, et al. Paeonol inhibits NLRP3 mediated inflammation in rat endothelial cells by elevating hyperlipidemic rats plasma exosomal miRNA-223. *Eur J Pharmacol.* 2020;885:173473.
15. Haneklaus M, O'Neill LA, Coll RC. Modulatory mechanisms controlling the NLRP3 inflammasome in inflammation: recent developments. *Curr Opin Immunol.* 2013;25:40–45.
16. Ren Y, Feng J, Lin Y, et al. MiR-223 inhibits hyperosmolarity-induced inflammation through downregulating NLRP3 activation in human corneal epithelial cells and dry eye patients. *Exp Eye Res.* 2022;220:109096.
17. Kim YJ, Yeon Y, Lee WJ, et al. Comparison of microRNA expression in tears of normal subjects and Sjögren syndrome patients. *Invest Ophthalmol Vis Sci.* 2019;60:4889–4895.
18. Qu M, Qi X, Wang Q, et al. Therapeutic effects of STAT3 inhibition on experimental murine dry eye. *Invest Ophthalmol Vis Sci.* 2019;60:3776–3785.
19. Yamaguchi T. Inflammatory response in dry eye. *Invest Ophthalmol Vis Sci.* 2018;59:Des192–Des199.
20. Rouen PA, White ML. Dry eye disease: prevalence, assessment, and management. *Home Healthc Now.* 2018;36:74–83.

Investigative Ophthalmology & Visual Science

21. Messmer EM. The pathophysiology, diagnosis, and treatment of dry eye disease. *Dtsch Arztebl Int.* 2015;112:71–81; quiz 82.
22. Ræder S, Klyve P, Utheim TP. Dry eye disease – diagnosis and treatment [in Norwegian]. *Tidsskr Nor Laegeforen.* 2019;139:752.
23. Thacker M, Sahoo A, Reddy AA, et al. Benzalkonium chloride-induced dry eye disease animal models: current understanding and potential for translational research. *Indian J Ophthalmol.* 2023;71:1256–1262.
24. Kim YH, Jung JC, Jung SY, Yu S, Lee KW, Park YJ. Comparison of the efficacy of fluorometholone with and without benzalkonium chloride in ocular surface disease. *Cornea.* 2016;35:234–242.
25. Jeon D, Jun I, Lee HK, et al. Novel CFTR activator Cact-3 ameliorates ocular surface dysfunctions in scopolamine-induced dry eye mice. *Int J Mol Sci.* 2022;23:5206.
26. Maruoka S, Inaba M, Ogata N. Activation of dendritic cells in dry eye mouse model. *Invest Ophthalmol Vis Sci.* 2018;59:3269–3277.
27. Zhang W, Li W, Zhang C, et al. Effects of vitamin A on expressions of apoptosis genes bax and Bcl-2 in epithelial cells of corneal tissues induced by benzalkonium chloride in mice with dry eye. *Med Sci Monit.* 2019;25:4583–4589.
28. Wang H-H, Chen W-Y, Huang Y-H, et al. Interleukin-20 is involved in dry eye disease and is a potential therapeutic target. *J Biomed Sci.* 2022;29:36.
29. Zhao W, Sun W, Li S, et al. Exosomal miRNA-223-3p as potential biomarkers in patients with cerebral small vessel disease cognitive impairment. *Ann Transl Med.* 2021;9:1781.
30. Li G, Zong X, Cheng Y, et al. miR-223-3p contributes to suppressing NLRP3 inflammasome activation in Streptococcus equi ssp. zooepidemicus infection. *Vet Microbiol.* 2022;269:109430.
31. Wan L, Yuan X, Liu M, Xue B. miRNA-223-3p regulates NLRP3 to promote apoptosis and inhibit proliferation of hep3B cells. *Exp Ther Med.* 2018;15:2429–2435.
32. Ren Y, Feng J, Lin Y, et al. MiR-223 inhibits hyperosmolarity-induced inflammation through downregulating NLRP3 activation in human corneal epithelial cells and dry eye patients. *Exp Eye Res.* 2022;220:109096.
33. Fan J, Bellon M, Ju M, et al. Clinical significance of FBXW7 loss of function in human cancers. *Mol Cancer.* 2022;21:87.
34. Yumimoto K, Nakayama KI. Recent insight into the role of FBXW7 as a tumor suppressor. *Semin Cancer Biol.* 2020;67:1–15.
35. Zhan T, Wang B, Fu J, et al. Artesunate inhibits Sjögren's syndrome-like autoimmune responses and BAFF-induced B cell hyperactivation via TRAF6-mediated NF-κB signaling. *Phytomedicine.* 2021;80:153381.
36. He J, Song Y, Li G, et al. Fbxw7 increases CCL2/7 in CX3CR1hi macrophages to promote intestinal inflammation. *J Clin Invest.* 2019;129:3877–3893.
37. Zhang L, Yang J, Guo M, Hao M. MiR-223-3p affects myocardial inflammation and apoptosis following myocardial infarction via targeting FBXW7. *J Thorac Dis.* 2022;14:1146–1156.
38. Liu S, Wang L, Wu X, Wu J, Liu D, Yu H. Overexpression of hsa_circ_0022742 suppressed hyperglycemia-induced endothelial dysfunction by targeting the miR-503-5p/FBXW7 axis. *Microvasc Res.* 2022;139:104249.
39. Balamurugan K, Sharan S, Klarmann KD, et al. FBXW7α attenuates inflammatory signalling by downregulating C/EBPδ and its target gene Tlr4. *Nat Commun.* 2013;4:1662.
40. Zhou YP, Xia Q. Inhibition of miR-103a-3p suppresses lipopolysaccharide-induced sepsis and liver injury by regulating FBXW7 expression. *Cell Biol Int.* 2020;44:1798–1810.
41. Liu Y, Peng J, Sun T, et al. Epithelial EZH2 serves as an epigenetic determinant in experimental colitis by inhibiting TNFα-mediated inflammation and apoptosis. *Proc Natl Acad Sci USA.* 2017;114:E3796–E3805.

Investigative Ophthalmology & Visual Science